第 49 卷 第 1 期
2022 年 1 月

湖南大学学报（自然科学版）
Journal of Hunan University (Natural Sciences)

Vol. 49 No. 1
January 2022

Open Access Article https://doi.org/10.55463/issn.1674-2974.49.1.21

Application of Error Correction Codes RS and LDPC to Enhance the Dicode Pulse Position Modulation

Yasmeen M. Hussein[1]*, Basman M. Al-Nedawe[2], Ammar Hussein Mutlag[1], Ameer K. Jawad[3]

[1] Electrical Engineering Technical College, Middle Technical University, Baghdad, Iraq

[2] Technical Institute of Baquba, Middle Technical University, Diyala, Iraq

[3] Department of Electric Engineering, Faculty of Engineering, Razi University, Kermanshah, Iran

Abstract: Dicode Pulse Position Modulation (DiPPM) has been presented as a new coding technique with several improvements over earlier PPM formats. Few analyses and experimental results have been published because it is a new coding scheme. To overcome the problem of bandwidth utilization in current PPM formats, DiPPM can be employed. The line rate is twice as fast as the original data rate. In order to increase DiPPM's error performance, two types of Forward Error Correction (FEC) codes, Reed-Solomon (RS) code and low-density parity-check (LDPC) code, are investigated in this article. When RS and LDPC function at their optimal parameters, the results show an improvement in DiPPM system error performance. The error performance of an uncoded DiPPM system was compared to that of a DiPPM-encoded LDPC system and a system utilizing the Reed-Solomon algorithm. Transmission efficiency is measured by the number of photons per pulse and bandwidth widening. When the bandwidth is 1x103 times or more than the initial data rate, DiPPM with LDPC code exceeds uncoded DiPPM and DiPPM with RS, using 1.821 x 103 photons per pulse, with a codeword length of 27 and code rate of 0.75.

Keywords: dicode pulse position modulation, forward error correction, low-density parity-check code, Reed-Solomon code.

纠错码 RS 和低密度脂蛋白在增强二码脉冲位置调制中的应用

摘要：二码脉冲位置调制 (迪 PPM) 已作为一种新的编码技术提出，与早期的 PPM 格式相比有一些改进。由于它是一种新的编码方案，因此很少发表分析和实验结果。为了克服当前 PPM 格式中的带宽利用问题，可以采用迪 PPM。线路速率是原始数据速率的两倍。为了提高迪 PPM 的错误性能，本文研究了两种类型的前向纠错 (前向纠错) 码，里德-所罗门 (RS) 码和低密度奇偶校验 (低密度脂蛋白) 码。当 RS 和低密度脂蛋白在其最佳参数下运行时，结果显示迪 PPM 系统错误性能有所改善。将未编码的迪 PPM 系统的错误性能与迪 PPM 编码的低密度脂蛋白系统和使用里德-所罗门算法的系统进行了比较。传输效率是通过每个脉冲的光子数和带宽加宽来衡量的。当带宽为初始数据速率的 1x103 倍或更多时，采用低密度脂蛋白码的迪 PPM 超过未编码的迪 PPM 和采用 RS 的迪 PPM，每脉冲使用 1.821 x 103 个光子，码字长度为 27，码率为 0.75。

关键词：二码脉冲位置调制、前向纠错、低密度奇偶校验码、里德-所罗门码。

Received: October 13, 2021 / Reviewed: November 18, 2021 / Accepted: December 15, 2021 / Published: January 28, 2022

About the authors: Yasmeen M. Hussein, Electrical Engineering Technical College, Middle Technical University, Baghdad, Iraq; Basman M. Al-Nedawe, Technical Institute of Baquba, Middle Technical University, Diyala, Iraq; Ammar Hussein Mutlag, Electrical Engineering Technical College, Middle Technical University, Baghdad, Iraq; Ameer K. Jawad, Department of Electric Engineering, Faculty of Engineering, Razi University, Kermanshah, Iran

Corresponding author Yasmeen M. Hussein, bbc0030@mtu.edu.iq

1. Introduction

A transmission medium, such as wired and wireless paths, or a transmission channel is incorporated into a communication device to enable the conveyance of data from a source to a receiver. In this process, the major parameters determining the trustworthiness of collected data are the channel and, more specifically, the external noise affecting it. Essentially, noise is the primary cause of signal interference and errors in data transmission. Channel coding is a smart way to increase interface performance in low-turbulence situations. In this regard, various pulse position modulation (PPM) formats, such as multiple PPM (MPPM) and differential PPM (DPPM), have been presented in the literature as coding schemes for optical communication. PPM is widely used in deep-space optical communication because of its high energy consumption, good anti-interference efficiency, and high detection frequency. However, one of its most significant disadvantages is that it produces an exceptionally high final data rate as a result of a large bandwidth expansion factor [1]. In other words, the final line rate may be extremely high, thereby restricting the usefulness of PPM. Accordingly, the aforementioned coding schemes are appropriate for synthesizing directed line-of-sight networks made of glass optical fiber cables, where bandwidth is inessential. Optical fiber connections are extensively employed in low-bandwidth magnetic recording networks given that they are inexpensive. To resolve the challenge presented by bandwidth, Sibley [4] developed dicode PPM (DiPPM) as an unconventional coding scheme with characteristics that surpass those of previously proposed PPM methods. More specifically, DiPPM was developed to eliminate the main concern of bandwidth dissipation via PPM.

Low-density parity-check (LDPC) codes are extensively used as codes that are more efficient than other adaptable codes because of their application in competent and reliable information transfer over bandwidth links in the presence of corrupting noise. Such codes can therefore function across a wide range of channels. The problem is that their reliability and accuracy, as well as the techniques that involve their usage, deteriorate as block length decreases. Only data transformations are sent via this signaling format, and no signal is transmitted when fixed data are conveyed.

LDPC and PPM demodulation based on iterative systems are popularly used as components of algorithms for deep-space optical communication because their output is close to the Shannon limit. Under a given noise level, when a communication channel is subjected to random data transmission errors, the Shannon limit refers to the highest volume of error-free data that can be transferred across the channel.

The error sources of DiPPM are controlled using the Reed–Solomon (RS) code, which was invented by Irving Reed and Gustave Solomon in 1960 [2]. The authors confirmed the superiority of DiPPM in efficiently checking errors, even as performance measured on the basis of the packet error rate can be enhanced using the RS algorithm at the time of error detection [2]. DiPPM errors acquired during transmission can also be eliminated using a maximum likelihood sequence detection (MLSD) error corrector [3]. Additionally, Basman M. Al-Nedawe [3] suggested that the RS code can overcome DiPPM error sources, significantly minimizing the number of errors that occur during transmission.

The current study is the first to propose an LDPC code as a solution to error sources that plague DiPPM. When employed with a DiPPM system, the optimal parameters of the LDPC code were discovered. An uncoded DiPPM system was compared with a coded DiPPM system employing the RS code in terms of photons per pulse and transmission efficiency. To the best of the authors' knowledge, DiPPM and LDPC code decoding techniques have not been examined as a means of mitigating the issue of bandwidth expansion in PPM. The present research intends to resolve this challenge by incorporating the proposed LDPC code into a DiPPM system to eliminate errors and investigate the optimum parameters of LDPC.

2. Dicode pulse position modulation

DiPPM was established to surpass PPM, wherein difficulties related to bandwidth expansion occur [4]. The former is similar to the latter in that they follow the same format patterns. In a single time interval amplification using pulse code modulation (PCM) in DiPPM, four time slots were used. PCM was used to digitally represent sampled analog signals, whose amplitude was measured at regular intervals for a PCM stream. Each sample was then calculated to the nearest value within a range of digital steps. The first and second slots each received a SET (S) pulse. The second slot was intended for a RESET (R) pulse, whereas the third and fourth slots were designed for intersymbol interference protection (ISI). Inverting PCM data from 0 to 1 produced the S pulse, whereas inverting one-to-zero data created the R pulse. This process is shown schematically in Fig. 1. Specifically, the figure illustrates PCM data translation from the top trace to the middle trace of a dicode and the bottom trace of DiPPM. The representations of DiPPM symbols is shown in Table 1.

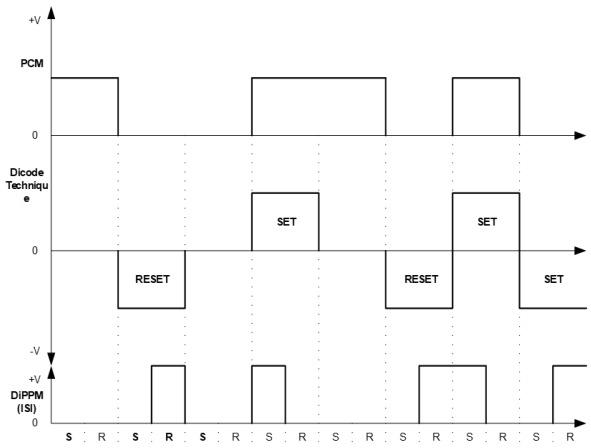

Fig. 1 Translation of top trace (PCM data) into middle trace (Dicode) and bottom trace (DiPPM)

Table 1 DiPPM symbol alphabet

PCM	DiPPM	Symbol
00	No pulse	N
01	SET	S
10	RESET	R
11	NO Pulse	N

Although the PCM data remained unchanged, no pulse was transmitted. However, because central decision detection was used to replace the slope detection technique, intersymbol interference was reduced. Using a basic first-order preamplifier in cascade and a third-order Butterworth filter, the central decision detection technique reduced the difficulty confronting the DiPPM decoder. The DiPPM's line rate was reduced to double that of actual real data because of the lack of guard bits. As a result, the considerable efficacy and simplicity of the DiPPM format led to the reasonable conclusion that it can compete with existing PPM formats used in optical fiber networks.

3. DiPPM Errors

Three types of detection errors can be found in the DiPPM format: wrong slots, erasure, and false alarm [5]. The next sections highlight the description and probabilities of these errors in detail.

3.1. Wrong-Slot Errors

A wrong-slot error occurs when noise on the rising edge of a recorded pulse causes the pulse to appear in consecutive time slots. Therefore, the pulse must be identified to reduce these errors in the middle of a Ts-width time slot. Moreover, a new pattern forms when the edge is transferred via [Ts/2]. P_{es}, which appears in the preceding slot, represents the probability of an error. It is presented by

$$P_{es} = 0.5 erfc\left(Q_{es} / \sqrt{2}\right) \quad (1)$$

Here, Q_s is given by:

$$Q_{es} = \left[T_s slope\left(t_d\right)\right] / \left[2\sqrt{n_o^2}\right] \quad (2)$$

where n_o^2 indicates the receiver's mean square noise, and slope (t_d) reflects the slope of the pulse received at the time of crossing the threshold, marked at t_d.

3.2. Erasure Errors

Errors in pulse erasure occur when the peak signal voltage falls below the threshold. This happens most often when there is a lot of noise. The likelihood of an error, which is denoted by P_{er}, can be calculated as follows:

$$P_{er} = 0.5 erfc\left(\frac{Q_{er}}{\sqrt{2}}\right). \quad (3)$$

Here,

$$Q_{er} = \left(v_{pk} - v_d\right) / \sqrt{n_o^2}\,, \quad (4)$$

where v_d is the voltage of the threshold crossing and v_{pk} is the voltage of the peak signal at the receiver's output.

3.3. False-Alarm Errors

When noise in an unused data slot exceeds a threshold limit, false-alarm problems arise. This error's probability, P_t, is calculated as follows:

$$P_t = 0.5 erfc\left(\frac{Q_t}{\sqrt{2}}\right), \quad (5)$$

where

$$Q_t = v_d / \sqrt{n_o^2}\,. \quad (6)$$

For each time slot, the number of uncorrelated samples can be determined as T_s/ϕ_R, where τ_R represents the time when the autocorrelation function in the receiver's filter becomes extremely small. The chance of a false alert P_f is calculated as follows:

$$P_f = \frac{T_s}{\tau_R} 0.5 erfc\left(\frac{Q_t}{\sqrt{2}}\right). \quad (7)$$

4. Reed–Solomon codes

These codes have a tremendous amount of power and utility. The codes are now widely utilized in a variety of applications because of the benefits they give, particularly in wireless communications systems [6].

- The Reed–Solomon codes have several basic characteristics: they are non-binary cyclic and made up of m-bit sequences, where m is any positive number greater than 2.
- There are associated symbols for the Reed–Solomon codes in the m-bit symbols.
- n and k are examples of systems that can be described as

$$0 < k < 2^m + 2\,. \quad (8)$$

The k in this situation refers to the amount of symbols in the data that are decoded using Reed–Solomon codes throughout the data transmission

procedure. The value n_{RS} denotes the total number of symbols in the code block's contained codes.

It is possible to acquire the highest code possible while crossing the lowest distance using Reed–Solomon codes (d_{min}) from the encoder input and output system for any code in the linear position.

Reed Solomon is a well-known novelist who has codes that can repair t or fewer combinations of communication channel faults, which are represented as follows:

$$t = [(d_{min} - 1)/2] = [(n - k)/2] \quad (9)$$

Fig. 2 depicts a typical Reed-Solomon code system.

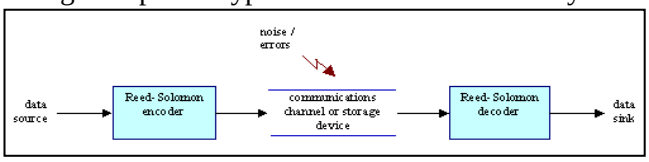

Fig. **Ошибка! Текст указанного стиля в документе отсутствует.** System of Reed-Solomon code

5. Encoding and Decoding by Reed Solomon

The encoding equation for the Reed-Solomon codes is:

$$(n.k) = (2^m - 1.2^m - 1 - 2t) \quad (10)$$

where $n-k = 2t$ denotes the number of parity symbols, and t denotes the Reed-Solomon code's symbol-error-correcting capabilities.

The following equation is the generating polynomial for a Reed-Solomon code.

$$g(X) = g_0 + g_1X + g_2X^2 + \cdots + g_{2t-1}X_{2t-1} + X^{2t} \quad (11)$$

The Bose, Chaudhuri, and Hocquenghem (BCH) codes, created by Irving Reed and Gus Solomon, represent the Reed-Solomon codes. The Reed-Solomon codes can be decrypted systematically as well. The systematic technique was identical to the binary encoding procedure since these codes are cyclic. A message polynomial, m(X), could be thought of as shifting into the codeword register stages (denoted by k) and then adding a parity polynomial (denoted by p) in this example (x). The far-left phases are represented by the letters n-k, which is the most common occurrence. Multiply the message polynomial by Xn-k to shift the message polynomial. The following equation can be obtained by dividing it by g(X), the generating polynomial:

$$X^{n-k}m(X) = q(X)g(X) + p(X) \quad (12)$$

where $q(X)$ and $p(X)$ are polynomials with quotient and remainder, respectively.

The early scholars' perspectives and analyses can also decode the Reed-Solomon codes. The codewords involved in the communication signal are corrupted during transmission due to system errors [6].

6. Low-Density Parity-Check (LDPC) Code

The Low-Density Parity-Check (LDPC) code is based on a parity search matrix of N columns and M rows, represented as H = [HMxN]. LDPC code has many 0s and a small number of 1s. In other words, distinctive traits have been deliberated into systematic LDPC codes. Each column has a fixed "1" number (i.e., column weight), and each row has a fixed "1" number, according to the criterion (i.e., the weight of the row). On the other hand, the column and line weights are not consistent. The LDPC code is a set of rules that has been defined by the LDPC code (N,y, k). The letters N stand for recurring, use a different codeword term length, and j, k stand for the column and row weights of the LDPC code, respectively. 1-y / k = 1-M / N is the LDPC code rate. The parity-check matrix with an 8-bit coding length is [7].

$$H = \begin{matrix} v_1 v_2 \cdots\cdots\cdots v_x \\ \begin{bmatrix} 0\,1\,0\,1\,1\,0\,0\,1 \\ 1\,1\,1\,0\,0\,1\,0\,0 \\ 0\,0\,1\,0\,0\,1\,1\,1 \\ 1\,0\,0\,1\,1\,0\,1\,0 \end{bmatrix} \begin{matrix} c_1 \\ c_2 \\ \vdots \\ c_y \end{matrix} \end{matrix}$$

, x = 1, 2, … N and y = 1, 2, ….., M

The Tanner graph has check node sets and variable nodes that correspond to each matrix row and column in a different H matrix setup (Fig. 3).

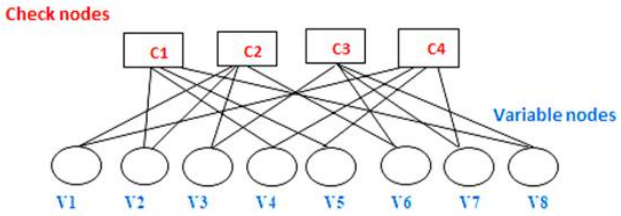

Fig. 3 A graphical representation of LDPC codes

6.1. Encoder

The encoder converts information bits into codewords using the generating matrix. The parity check matrix and the generator are presumed to be connected. The parity check matrix listed below will be delivered in a standard format [8]:

$$H = [A|I_{n-k}] \quad (13)$$

and generator matrix is:

$$G = [I_k|A^T] \quad (14)$$

As follows, a codeword C will be generated:

$$C = UG \quad (15)$$

U denotes a block associated with the information bits, while G denotes the generating matrix. The following is a list of valid code words to check:

$$HC^T = 0 \quad (16)$$

where $(.)^T$ The transpose matrix is represented as. If the result of (16) is non-zero, C will be invalid, and the error repair technique will also be used in this case.

6.2. Decoder

There are two types of judgments in the iterative parity check decoder: hard and soft. The Sum-Product Method (SPA) is a soft choice message-passing system in which each received bit's input reflects the likelihood of previous channel information. The three forms of SPA based on the message structure between variable and check nodes are Probability Domain, Log Domain,

and Min-Sum SPA. The Min-Sum technique outperformed the Log Domain and Prob. Domain algorithms by a significant amount of the Signal to Noise Ratio (SNR). Finally, based on the excellent results, the optimum LDPC parameter values were determined [8].

7. Simulation

A system model tries to imitate some of the characteristics of a system. The central detection strategy was used to detect the received signal. A white-noise spectrum at an optical receiver's output with a narrow bandwidth, wc, was used in the simulation. As the receiver's spectrum was white noise, the pre-detection filter was a standard matching filter. The signal supplied to the threshold detector was examined when DiPPM was routed through graded-index POF [9].

$$v_o(t) = bзqR_T \frac{ш_c}{2} exp(\acute{о}^2 ш^2) \times exp(- ш_c t) erfc[\acute{о} ш_c - (\frac{t}{2\acute{о}})] \quad (17)$$

з is the detector's quantum efficiency, q is the electronic charge, R_T is the receiver's mid-band trans-impedance, and щ is the change of the Gaussian pulse obtained, $ш_c$ number of per column, б is the fiber bandwidth.

$$б = \frac{0.1874 T_b}{f_n} \quad (18)$$

T_b is the bit-time of PCM, and f_n is the fibre bandwidth normalized to the PCM data rate. (n_o) signifies the noise performing on the signal as given in the context of Eq. 19.

$$\langle n_o^2 \rangle = S_o \frac{ш_c}{2} R_T^2 \, exp(\acute{о}^2 ш_c^2) erfc(\acute{о} ш_c) \quad (19)$$

where So on both sides is the current spectral density of the preamplifier's equivalent input-noise current. It was decided to use a PIN photodiode because of its low shot noise. The time when the noise at the filter's output's autocorrelation function becomes minimal has been calculated as $\tau_R=\alpha$. The threshold level, v, was utilized as a system variable, and it was specified as follows:

$$v = \frac{v_d}{v_{pk}} \quad (20)$$

where v_{pk} is the isolated pulse's peak voltage and v_d is the threshold crossing voltage.

Two types of Forward Error Correction (FEC) codes, firstly, Reed-Solomon code, are especially helpful for detecting and repairing burst mistakes. This is partly due to the great efficiency of these codes for memory-based communication routes. When the input symbols for the channels are huge, the usage of codes is also advantageous**.**

In the context of the potential of a symbolic channel error, the Reed-Solomon symbol error probability E can be demonstrated:

$$P_E \approx \frac{1}{2^m - 1} \sum_{j=t+1}^{2^m - 1} j \binom{2^m - 1}{j} p^j (1-p)^{2^m - 1 - j} \quad (21)$$

With the formula below, the symbol error probability is related to the binary error probability P_{eb}.

$$P_{eb} = \frac{2^{M-1}}{2^M - 1} P_E \quad (22)$$

The second type distribution of the channel log-likelihood ratio (LLR) is used to analyze LDPC codes. The channel LLR L is frequently measured by supposing the code words are all zeros. (x = +1) was conveyed, and L is expressed as

$$L = \log \frac{p(x=+1|y)}{p(x=-1|y)} \quad (23)$$

The average bit error probability distribution for the finite-length case is computed by considering the N samples from the symmetric Gaussian LLR distribution. In this regard, each sample or bit is incorrect within negative LLR. Accordingly, the likelihood of error of each sample (Fpobs) is mathematically defined on x in the following equation (Eq. 24). In this regard, the summation of all corresponding errors divided by N would signify the probability of errors [8].

$$Fp_{obs}(x) = \binom{N}{Nx} p_o^{Nx} (1 - p_0)^{N-Nx} \quad (24)$$

N x is an integer, and $0 \le N x \le N$. However, The Fpobs is approximated defined by a Gaussian pdf $N(p_0, p_0(1p_0)/N)$ with insignificant values for x outside [0, 1] for large N[1].

The pulse shape and noise may be approximated for a particular fiber bandwidth. The ideal value of v that produces the least amount of photons per pulse, b, can be discovered for a given PCM error rate (1 in 10^9 in the simulations). With a wavelength of 650 nm and a photodiode quantum efficiency of 100%, a 1 Gbit/s PCM data-rate device was investigated. Compared to the input, the preamplifier had a bandwidth of 10 GHz and white noise of 50 x 10^{-24} A 2 /Hz. A commercial instrument was used to take these measurements. n=10 was achieved using line-coded PCM data. DiPPM systems with and without RS coding were employed in the simulations. The DiPPM transmission efficiency, both uncoded and coded, is about the same. The transmission efficiency of uncoded and coded DiPPM can be described as (25) and (26), respectively.

$$c \frac{= \ln 2}{b} \quad (25)$$

$$c \frac{= r \ln 2}{b} \quad (26)$$

Uncoded DiPPM transmission efficiency is shown in equation (25), where b is the number of photons, but DiPPM transmission efficiency is shown in equation (26) when RS and LDPC codes are used. The coding rate r affects the system's transmission. On the other hand, using RS code and LDPC code at the appropriate code rate reduces the number of photons, enhancing total transmission efficiency.

8. Rustle

The data in these images use a codeword length of 2^M to calculate the number of photons, where M=3,4,5,6,7. It is worth noting that as the RS code rates increase, so does the number of photons. This is the case because the RS coding speeds are related to the number of data symbols. In addition, when using the slope detection approach, the number of photons is proportional to the normalized bandwidth.

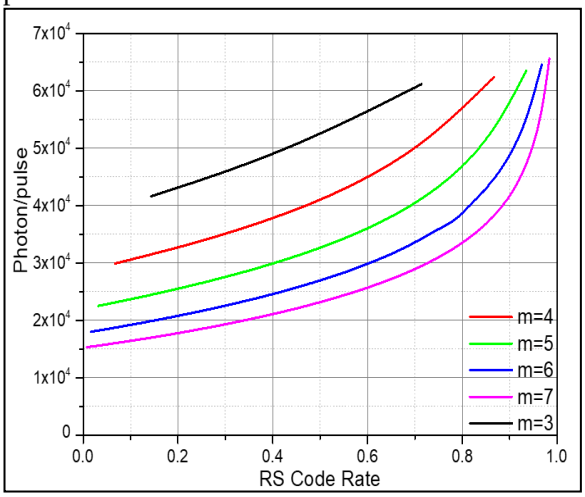

Fig. 4 Variation of photons' number against RS code rate at different normalized bandwidths

A coding rate of roughly 3/4 is suitable for achieving maximum transmission efficiency. As predicted by the equation, the amount of redundant symbols grows, and performance worsens when the DiPPM coding system is not performing at its best (25). As the ideal coding rate is exceeded, the number of redundant symbols drops, meaning that the number of corrective symbols falls, diminishing transmission efficiency.

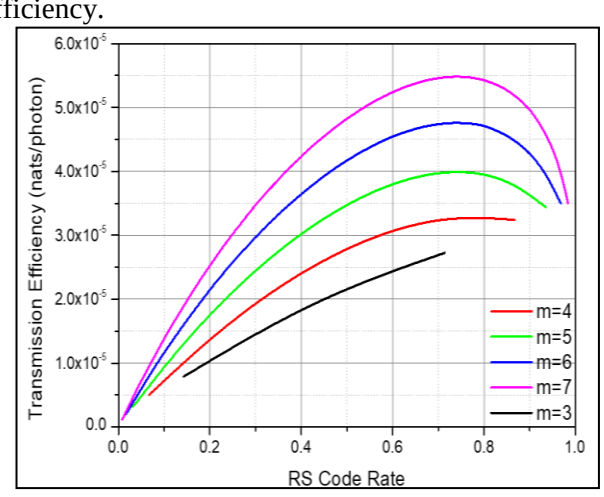

Fig. 5 Transmission efficiency versus RS code rate at different normalized bandwidth

This section aims to discuss the impact of the number of photons per pulse (b) in the DiPPM-coded format while using slope and central detection systems at various code speeds. A 2M codeword length is used to calculate the number of photons, using M values ranging from 3 to 7. It is vital to remember that as the LDPC code rate rises, b rises with it. This is due to a consistent relationship between the number of data symbols and the LDPC code rates. When employing the slope detection procedure, b is proportional to the normalized bandwidth. This is also owing to the slope detection approach's dependency on the established signal's shape.

The fluctuation of b for a DiPPM system utilizing LDPC against the LDPC coding rate at different normalised bandwidths is shown in Fig. 6. At varied LDPC code speeds and normalised bandwidths, the least number of photons appears to be established. It is worth noting that the system's mistake rate was kept to a bare minimum. More importantly, b is inversely proportional to the number of normalised bandwidths. The lowest b values are validated for the maximum normalized bandwidth. In addition, as the LDPC code rate increases, b increases exponentially. Hence, it is critical to recognize the significance of reducing b to the appropriate gene. In this regard, it is vital to perceive the importance of mitigating b to accordingly generate the optimal code rate in the application of an LDPC code and to accelerate the highest performance of the device.

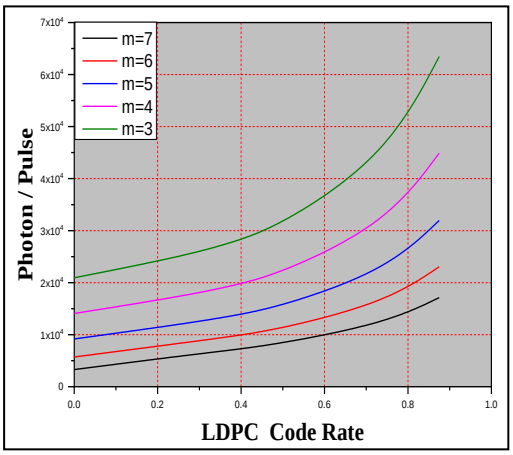

Fig. 6 Number of photons against LDPC code rate at different normalized bandwidths

The transmission efficacy of the coded DiPPM system against LDPC coding rates for multiple fiber normalised bandwidths is shown in Fig. 7. For the largest normalised bandwidths, Fig. 7 confirms an optimum transmission efficacy of around 0.6 of the LDPC coding rate. However, at lower normalised bandwidths, the best transmission efficacy is found at higher LDPC coding rates of around 0.7. It is critical to recognize that the transmission efficacy and the code rate have an exponential relationship because the efficacy is essentially diminished after reaching the ideal code rate. In other words, while the code rate has increased, the number of uncoded symbol errors has increased even more. As a result, the system's efficacy and the transmission of corrected symbols are diminished. In this case, the level of redundancy and the rate of redundancy rise over the ideal coding rate.

Higher fiber normalized bandwidths, on the other hand, successfully increase transmission efficacy.

Fig. 7 and 8 demonstrate the importance of lowering b with LDPC codes to enhance the transmission efficiency of the DiPPM.

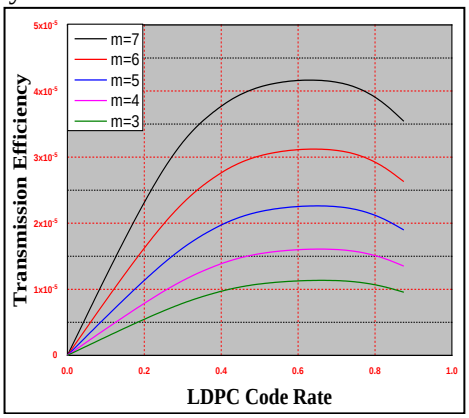

Fig. 7 The transmission efficacy of coded DiPPM system against LDPC code rates within different normalized bandwidths

Fig. 8 demonstrates the variation of the number of photons per pulse for the coded PCM system against LDPC Code Rate for several normalized fiber bandwidths (f_n). It can be stated that there is a direct positive relationship between the number of photons per pulse and the LDPC code rate for any selected normalized bandwidth. Specifically, the number of photons increases with an increase in code rate for a particular bandwidth.

Fig. 9 illustrates the relationship between the transmission efficiency of PCM employing the LDPC code system against the LDPC code rate for various fiber bandwidths (f_n) normalized to the PCM data rate. It can be concluded that employing an optimum value of 0.7 of the LDPC code rate would maximize the overall efficiency. The coded Dicode Pulse Position Modulation (DiPPM) using the LDPC code realizes the highest transmission efficiency for the low dispersive channel. This can be attributed to the bandwidth's expansion, which would consume more energy by adding the redundancy symbols. The process of calculating transmission efficiency for the PCM using the LDPC code system and relationship of Sibley [4] is carried out as follows:

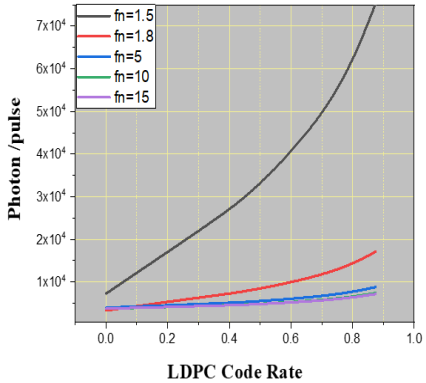

Fig. 8 Variation of photons' number against LDPC code rate at different normalized bandwidth

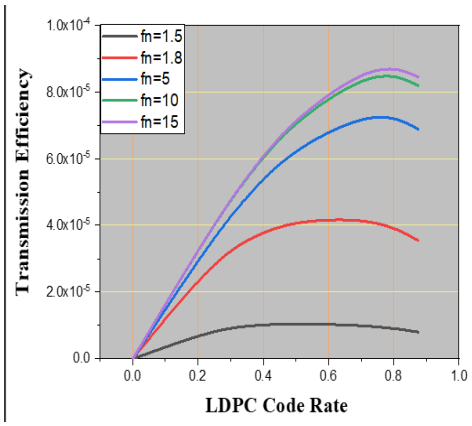

Fig. 9 Transmission efficiency versus LDPC code rate at different normalized bandwidth

Using these methods, Fig. 10 compares the number of photons in uncoded and coded DiPPM systems at various bit error rates. With a coding rate of roughly 3/4, the RS code length per codeword ranged from 15 to 128 symbols. Fig. 12 depicts the transmission efficiency of a DiPPM coded system with 31 RS symbols at various bit error rates. The results indicate that the RS has a slightly similar optimum code rate even when the system is working at a different bit error rate.

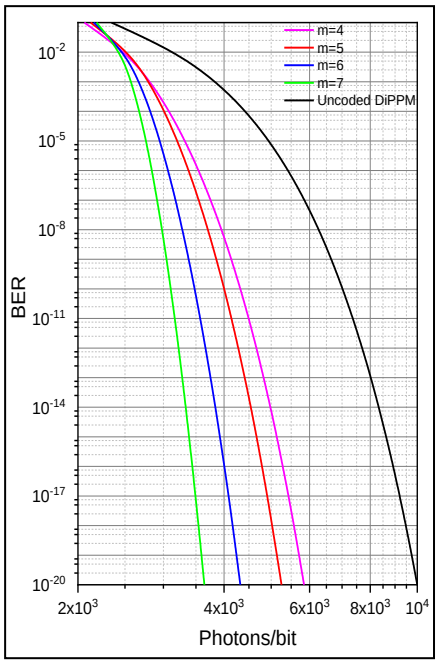

Fig. 10 BER vs. Q, the signal-to-noise ratio parameter, at BW=100 normalized

Codeword length and system bit error rate (BER) did not affect the optimum LDPC coding rate while raising the LDPC codeword length and lowering the BER improved system performance. On the contrary, the complexity of the LDPC system design is proportional to the codeword length, as illustrated in Fig. 11.

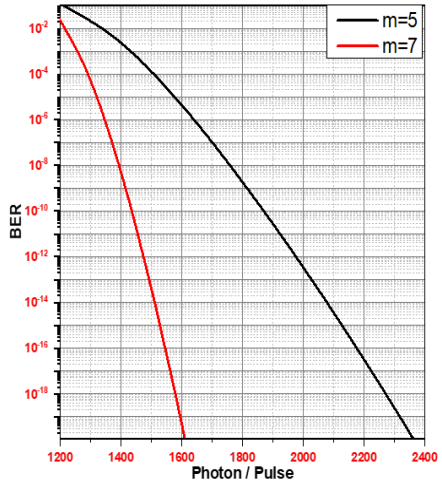

Fig. 11 BER vs. Q, the signal-to-noise ratio parameter, at BW = 100 normalized

When using a bandwidth of 0.9 times or greater than the PCM data rate, the LDPC algorithm requires only 1.821 x 103 photons per pulse, as shown in Fig. 10. The number of photons per pulse is lowered when the RS system works at a bandwidth of less than 1 MHz. When running at high bandwidth, the DiPPM with LDPC code system outperforms the DiPPM with RS system because the LDPC system expands the operational bandwidth of the DiPPM system based on the LDPC code rate.

Table 2 System with and without RS or LDPC in DiPPM

fn	Uncoded DiPPM	DiPPM with RS	DiPPM with LDPC
0.46	658.4 x 103	76.3 x 103	----
1	95.8 x 103	11.4 x 103	3.128 x 103
1.8	25.6 x 103	4.5 x 103	2.720 x 103
10	4.7 x 103	1.4 x 103	1.821x 103
100	2.1 x 103	0.9 x 103	0.975 x 103

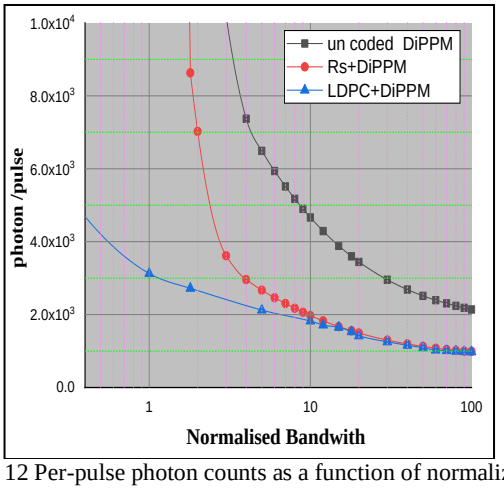

Fig. 12 Per-pulse photon counts as a function of normalized bandwidth

9. Conclusion

The number of photons required for each pulse, as well as the transmission efficiency and bandwidth expansion, were investigated in this work using RS codes and LDPC codes with DiPPM. The simulation findings show that reducing the number of photons with LDPC codes improves DiPPM transmission efficiency significantly. According to the data, the DiPPM coded system outperforms the uncoded system by 5.12db when running at the optimum coding rate of 3/4. Likewise, the system performance improves when the LDPC codeword is increased and BER is reduced. The findings reveal that the LDPC optimum code rate is unaffected by the system or type of code employed. Better results of using an LDPC code with DiPPM than those of using the RS code with DiPPM are shown.

References

[1] SKLAR B. *Digital Communications: Fundamentals and Applications.* 2nd ed. Prentice-Hall, New Jersey, 2001.

[2] REED I. S., & SOLOMON G. Polynomial codes over certain finite fields. *Journal of Applied Mathematics*, 1960, 8: 300-304. https://doi.org/10.1137/0108018

[3] AL-NEDAWE B. M., BUHAFA A. M., SIBLEY M. J., and MATHER P. J. Improving error performance of dicode pulse position modulation system using forward error correction codes. Proceedings of the 21st Telecommunications Forum Telfor, Belgrade, 2013, pp. 331-334. https://doi.org/10.1109/TELFOR.2013.6716237

[4] SIBLEY M. J. Dicode pulse-position modulation: a novel coding scheme for optical-fibre communications. *IEE Proceedings - Optoelectronics*, 2003, 150(2): 125-131. https://doi.org/10.1049/ip-opt:20030386

[5] CRYAN R. A., & SIBLEY M. J. Minimising intersymbol interference in optical-fibre dicode PPM systems. *IEE Proceedings - Optoelectronics*, 2006, 153(3): 93-99. https://doi.org/10.1049/ip-opt:20050028

[6] CRYAN R. A., & UNWIN R. T. Reed-Solomon coded homodyne digital pulse position modulation. IEE Proceedings I (Communications, Speech and Vision), 1992, 139(2): 140-146. https://doi.org/10.1049/ip-i-2.1992.0021

[7] HUSSEIN Y. M., MUTLAG A. H., and AL-NEDAWE B. M. Comparisons of Soft Decision Decoding Algorithms Based LDPC Wireless Communication System. *IOP Conference Series: Materials Science and Engineering*, 2021, 1105(1): 012039. https://doi.org/10.1088/1757-899X/1105/1/012039

[8] YAZDANI R., & ARDAKANI M. An efficient analysis of finite-length LDPC codes. Proceedings of the International Conference on Communications, Glasgow, 2007, pp. 677-682. https://doi.org/10.1109/ICC.2007.116

[9] SHU L., & COSTELLO D. J. Error Control Coding Fundamentals and Application. Prentice-Hall, London, 1983.

参考文:

[1] SKLAR B. 数字通信：基础和应用。第 2 版。新泽西州普伦蒂斯霍尔，2001 年。

[2] REED I. S. 和 SOLOMON G. 某些有限域上的多项式代码。应用数学杂志，1960，8：300-304。https://doi.org/10.1137/0108018

[3] AL-NEDAWE B. M.、BUHAFA A. M.、SIBLEY M. J. 和 MATHER P. J. 使用前向纠错码提高二码脉冲位置调制系统的误差性能。第 21 届特尔福电信论坛论文集，贝尔格莱德，2013 年，第 331-334 页。https://doi.org/10.1109/TELFOR.2013.6716237

[4] SIBLEY M. J. 二码脉冲位置调制：一种用于光纤通信的新型编码方案。独立外部评价程序- 光电子学, 2003, 150(2): 125-131。 https://doi.org/10.1049/ip-opt:20030386
[5] CRYAN R. A., & SIBLEY M. J. 最小化光纤双码 PPM 系统中的符号间干扰。独立外部评价程序- 光电子学, 2006, 153(3): 93-99 。 https://doi.org/10.1049/ip-opt:20050028
[6] CRYAN R. A. 和 UNWIN R. T. 里德-所罗门编码零差数字脉冲位置调制。独立外部评价诉讼我（交流、演讲和视觉）, 1992, 139(2): 140-146. https://doi.org/10.1049/ip-i-2.1992.0021
[7] HUSSEIN Y. M.、MUTLAG A. H. 和 AL-NEDAWE B. M. 基于低密度脂蛋白无线通信系统的软判决解码算法的比较。眼压会议系列：材料科学与工程, 2021, 1105(1): 012039. https://doi.org/10.1088/1757-899X/1105/1/012039
[8] YAZDANI R., & ARDAKANI M. 有限长度低密度脂蛋白码的有效分析。国际通信会议论文集，格拉斯哥，2007 年，第 677-682 页。 https://doi.org/10.1109/ICC.2007.116
[9] SHU L., & COSTELLO D. J. 错误控制编码基础和应用。普伦蒂斯霍尔，伦敦，1983 年。